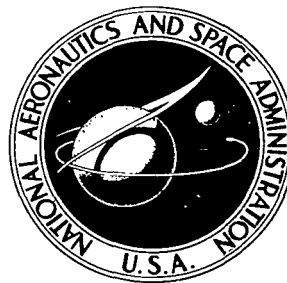


**NASA TECHNICAL NOTE**



**NASA TN D-7041**

*C.1*

**NASA TN D-7041**

**LOAN COPY: RETURN  
AFWL (DOGL)  
KIRTLAND AFB, NM**

0133627



**TECH LIBRARY KAFB, NM**

# **HOT ELECTRODE DROPS IN AN UNSEEDED SUPERSONIC ARGON MAGNETOHYDRODYNAMIC GENERATOR**

*by Maris A. Mantenieks*

*Lewis Research Center*

*Cleveland, Ohio 44135*

**NATIONAL AERONAUTICS AND SPACE ADMINISTRATION • WASHINGTON, D. C. • JANUARY 1971**



0133627

1. Report No. NASA TN D-7041	2. Government Accession No.	3. Recipient's Catalog No.	
4. Title and Subtitle HOT ELECTRODE DROPS IN AN UN- SEEDED SUPERSONIC ARGON MAGNETOHYDRODY- NAMIC GENERATOR		5. Report Date January 1971	
7. Author(s) Maris A. Manteniekis		6. Performing Organization Code	
9. Performing Organization Name and Address Lewis Research Center National Aeronautics and Space Administration Cleveland, Ohio 44135		8. Performing Organization Report No. E-5926	
12. Sponsoring Agency Name and Address National Aeronautics and Space Administration Washington, D. C. 20546		10. Work Unit No. 129-02	
		11. Contract or Grant No.	
15. Supplementary Notes		13. Type of Report and Period Covered Technical Note	
16. Abstract  Experiments were performed in an unseeded, supersonic argon generator. Floating potential profiles, electrode drops, and electrode temperatures were measured. The following conclusions were reached: (1) Electrode drops are independent of the magnetic field. (2) The discharge is not symmetrical in the presence of a magnetic field. (3) It is possible to go from a self-sustaining arc discharge mode to a non-self-sustaining mode by increasing the initial cathode temperature. (4) There is a cathode temperature (about 2250 K) for which a minimum cathode drop is found. (5) A cooling effect for low discharge current is observed at the cathode in the non-self-sustaining mode. This cooling depends on the magnetic field.		14. Sponsoring Agency Code	
17. Key Words (Suggested by Author(s)) Magnetohydrodynamics Plasma Electrode drops Power generator		18. Distribution Statement  Unclassified - Unlimited	
19. Security Classif. (of this report) Unclassified	20. Security Classif. (of this page) Unclassified	21. No. of Pages 23	22. Price* \$3.00

# HOT ELECTRODE DROPS IN AN UNSEEDED SUPERSONIC ARGON MAGNETOHYDRODYNAMIC GENERATOR

by Maris A. Mantenieks  
Lewis Research Center

## SUMMARY

Experiments were performed in an unseeded, supersonic, argon magnetohydrodynamic (MHD) generator. The generator contained a single electrode pair made of carbonized thoriated tungsten. The electrodes were inserted into the stream to ensure thermionic emission. Probes were placed in both sidewalls to measure floating potential profiles in the electrode gap and to measure electrode drops. Also electrode temperatures were measured. Data are presented for different mass flow rates and two magnetic field strengths (0.54 and 0.39 T).

The following conclusions were reached:

- (1) Electrode drops are independent of the magnetic field.
- (2) The discharge is not symmetrical in the presence of a magnetic field.
- (3) It is possible to go from a self-sustaining arc discharge mode to a non-self-sustaining mode by increasing the initial (i. e., zero discharge current) cathode temperature.
- (4) There is a cathode temperature (about 2250 K) for which a minimum cathode drop is found.
- (5) A cooling effect for low discharge current is observed at the cathode in the non-self-sustaining mode. This cooling depends on the magnetic field.

## INTRODUCTION

Electrode processes strongly influence the performance of a magnetohydrodynamic (MHD) generator. Large electrode drops can appreciably lower the generator efficiency. Electrode performance is governed by many factors including electrode material, surface conditions (e. g., seed coverage and foreign deposits), and the properties of the boundary layer (ref. 1). These factors are strongly influenced by electrode temperature.

In an MHD generator which uses "seed" to enhance the plasma conductivity and to provide the required cathode emission, electrode processes are obscured by the complicated relations at the electrode surface between the condensing seed and the plasma. A generator without seed offers a simpler picture of the electrode processes. A supersonic, arc-heated, nonequilibrium, argon MHD generator has been operated successfully (ref. 2) and was used for this electrode study. The results obtained using carbonized Th-W electrodes at different initial cathode temperatures are presented in this report.

## EXPERIMENTAL APPARATUS AND MEASUREMENTS

### Description of Apparatus

Arc heater and nozzle. - The arc heater is vortex-stabilized and consists of a  $1\frac{1}{8}$ -inch (32-mm) diameter, annular, water-cooled copper anode and a water-cooled thoriated tungsten cathode. The argon flows into the arc heater through tangential holes in a ceramic sleeve separating the anode from the cathode.

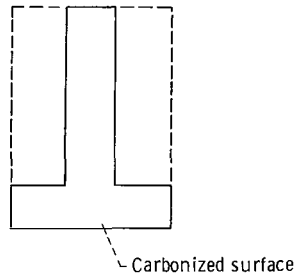
A water-cooled convergent-divergent copper nozzle with a throat diameter of 1.44 inches (3.65 cm) and an area ratio of 4.34 is used. The calculated Mach number at the nozzle exit, assuming isentropic expansion of a perfect gas, is 3.6.

Test section. - The test section is a 3.0-inch (7.6-cm) inside-diameter stainless-steel tube 14 inches (35.6 cm) long. Nine pure tungsten wire probes were placed on both sides of the test section in the direction of the magnetic field and perpendicular to the current path as shown in figures 1(a) and (b). The probes are equally spaced along the 3.8-centimeter electrode gap on each side of the test section.

Electrodes. - A good cathode must be a good emitter and must withstand the high temperature of the plasma. Thoriated tungsten (Th-W) satisfies these requirements fairly well and was previously used in a study of arc discharge characteristics in a MHD generator (ref. 3). However, thoriated tungsten suffers an irreversible loss of emission properties when it is heated above approximately 2000 K because of thorium depletion (ref. 4). Also oxygen on the surface may cause nonuniform emission if electrodes are not properly activated. Improved emission characteristics are obtained if the Th-W is carbonized. The carbonization process involves heating the sample to a high temperature ( $\sim 2200$  K) in a benzene vapor and hydrogen atmosphere. This process decreases the susceptibility to "poisoning" and eliminates the presence of oxygen on the surface which may change the work function considerably. Carbonization also retards thorium loss and therefore can provide more uniform emission at higher working temperatures (ref. 4). The work function of the carbonized electrode, however, still has to be de-

terminated, since the emission characteristics may vary with carbonizing temperature, benzene content in the hydrogen, and length of the carbonizing period (ref. 4).

The electrodes were fabricated from a Th-W (2 percent) cylinder which had been carbonized. Then the cylinder was electric-discharge machined to the shape shown in the following sketch, thus providing one carbonized surface of 0.11-square-inch (0.707-sq-cm) area.



The electrode then was crimped into a pure tungsten stem. (The tungsten stem had a hole machined in one end for the electrode to fit into.) The electrodes were inserted into the stream, away from the cold boundary layer at the wall, to ensure thermionic emission.

## Measurements

Argon plasma conditions (shown in table I). - The argon stagnation temperatures were calculated calorimetrically by measuring the power into the gas (the power into the arc minus the power lost by the cooling water) and dividing by the argon mass flow rate. The static temperature is determined by assuming an isentropic expansion through the nozzle. The small temperature differences in the cooling water proved difficult to measure accurately. Since the coolant water rate through the arc heater was very high, this error in the temperature readings could cause considerable error in the static temperature calculations. The error may be as large as  $\pm 15$  percent, but this should not be of major importance in the experiment (ref. 5). The most important parameter in this experiment is considered to be the electrode temperature, which was measured much more accurately.

MHD generator and instrumentation. - At the maximum magnetic field of 0.54 tesla, open-circuit voltages of about 21 volts (approximately one-half of theoretical value) and short-circuit currents up to 34 amperes were obtained.

Eight load resistances (including open circuit), each automatically timed for 2- to 4-second intervals, gave the V-I characteristics of the generator. Probe voltages as well as electrode voltages and other arc data were recorded for each load resistance value with a high-impedance ( $1\text{-M}\Omega$ ) automatic data recording device. All potential difference measurements presented in the data are measured with respect to the cathode.

Electrode temperature. - Electrode temperatures were measured by a two-color (wavelengths of 650 and 550 nm) pyrometer. The temperature is indicated on a meter calibrated in degrees, with a linear scale. Also a millivolt output is used to record the data so the temperature may be correlated to the current through the electrode.

The optical path for the pyrometer measurements included a quartz window and a mirror. Compared to a known temperature light source, this path introduced about a 1-percent error in the temperature measurement. It was found that during a run the quartz window did not discolor or lose its transparency.

To obtain the effect of the hot plasma on the temperature measurements the following steps were taken. Current was passed through a tungsten rod inserted in the plasma. The temperature of the rod was monitored continuously until enough current was passed through the rod to melt the tip. It was found that the measured melting point of the rod was within the 1-percent error of the listed melting point of tungsten. Thus the plasma had no appreciable effect on the temperature measurements.

## RESULTS AND DISCUSSION

### Floating Potential in Electrode Gap

Floating potential profiles with no induced or applied voltage across the electrodes are shown in figure 2(a). Because of the balance of the electron flux from the nonequilibrium plasma and the emitted electrons from the electrodes, the probes are at about a volt higher than the electrodes. (This condition is discussed in more detail in the appendix.) The shape of the profiles, in the vicinity of the electrodes, of the two grids is not the same. The corresponding end probe potentials (i. e., potential on probe 1 of grid A and the potential on probe 1 of grid B) differ by approximately 0.5 volt. This difference is not well understood. It may be due to plasma flow nonuniformity in the test section.

When voltage is applied and a discharge obtained between the electrodes, a similar voltage profile is obtained (fig. 2(b)). Again the end pins differ by about 0.5 volt.

Typical floating potential profiles for magnetically induced fields are presented in figures 3 and 4. In figure 3 the top electrode is the cathode and in figure 4 the bottom electrode is the cathode. Two magnetic field values were used, 0.54 tesla in figures 3(a)

and 4(a) and 0.39 tesla in figures 3(b) and 4(b). It is interesting to note that again the corresponding end probe potentials do not agree. The difference is not, however, 0.5 volt as noted before but gets as large as 4 volts for large currents at the anode of figure 3(a). Also the electric field as determined from the potential profiles in the center of the duct of both grids (fig. 5) is found to be consistently higher at grid A for both magnetic field directions. This indicates that the magnetic field (possibly in conjunction with the plasma nonuniformities mentioned before) causes a nonsymmetrical discharge current path.

The change of polarity of the magnetic field should have no effect upon the performance of the generator for the same plasma conditions. However, higher open-circuit voltages (20.4 V compared to 19.3 V) and higher short-circuit currents (34.1 A compared to 25.4 A) were found for the polarity of figure 3 compared to that of figure 4. Again nonuniformities in the plasma flow may account for this. The difference between the open-circuit values of the two polarities is proportional to the magnetic field strength.

## Electrode Drops and Temperature

The potential change near an electrode, usually called an electrode drop, is difficult to measure accurately because of the very small sheath thickness and the perturbations caused by the probe. However, the potential difference between the electrode and the probe nearest that electrode may yield an approximate value of the electrode drop. Because of the differences between the values from grids A and B, the drop was considered to be the average of the two measured voltages.

In this report a change of potential in layers adjacent to the electrodes is considered positive if the potential in the layer increases with reference to the electrode surface.

Cathode. - The cathode drops and corresponding cathode temperature against current are plotted in figure 6. The drops increase from about 1 volt for zero current to 10.2 volts for short-circuit conditions. At higher currents the drops become independent of the current. To observe the temperature effect of the cathodes, the cathode drops are plotted against cathode temperature for various load currents in figure 7. The initial cathode temperature (the value at zero load current) was increased by operating the arc heater at a decreased argon mass flow rate. Figure 7 shows that for a given current the cathode voltage drops decrease with cathode temperature and reach a minimum value at about 2250 K. Beyond this temperature the drops increase with increasing cathode temperature. The former effect is expected since the electrode emission improves with increasing temperature. Similar behavior has been observed by Musin (ref. 8) and Maslennikov and Germanyuk (ref. 9). The latter effect is most probably due to thoria depletion at the cathode surface. Schneider (ref. 4) has shown that thoria be-

gins to be depleted from a carbonized Th-W electrode at an appreciable rate beginning at about 2250 K, causing the work function to increase. A similar minimum voltage drop characteristic observed in a potassium-argon system is described in reference 10.

A decrease in the temperature of the cathode, with increasing current as seen in thermionic converters (ref. 11), is observed in figure 6 at low currents for higher initial cathode temperatures. This cooling effect is the result of the energy the electrons take from the cathode and increases with increasing initial cathode temperature. The maximum cooling  $\Delta T$  (defined as the difference between the zero-current temperature and the minimum temperature) is plotted against initial cathode temperature in figure 8. The figure shows that the  $\Delta T$  is a linear function of the initial temperature. The magnetic field effect on the cathode temperature observed in figure 6 is more pronounced in figure 8, indicating maximum cooling increasing with decreasing magnetic field.

Anode. - Anode drops with corresponding electrode temperatures are plotted against load current in figure 9. The drops increase negatively with increasing current, whereas the temperature increases linearly with increasing current. The negative drops are the largest for the lowest initial anode temperature and the smallest for the highest initial anode temperature.

Again there appears to be a small anode temperature difference between the high and low magnetic field cases, but no difference is observed for the anode drop.

## Model of Discharge

A discharge in a generator may operate in either a non-self-sustaining mode (i. e. , discharges utilizing separate heat sources for the cathode, such as heaters or the flowing plasma itself in our case) or a self-sustaining arc mode. A stable non-self-sustaining discharge is possible if the cathode is capable of maintaining a sufficiently high electron emission; if uniform emission is too low, the cathode can only provide the necessary emission from a constricted arc (self-sustaining mode, refs. 4 and 6). It is possible, as expected, to go from the one mode to the other by changing the initial cathode temperature.

From these observations about the current voltage characteristics and the corresponding cathode temperature behavior, one may suggest the following model of the discharge in this experiment. The discharge characteristics as observed in figure 6 may be divided into two regions: (1) a low current region where the drops increase with increasing current, exhibiting a cooling effect; and (2) a high current region where drops are more or less independent of current and the temperature increases with increasing current. It might be surmised that in the low current region the discharge is dominated



by electron current and the drop is dependent on a balance of emitted electron current and the electron flux from the plasma. As the current increases, the cathode is not able to supply the required number of electrons and an ionization region is formed to provide ions, which are accelerated by the same drop to heat the cathode. When a sufficiently high ion density is created due to the space-charge neutralization, a transition from the non-self-sustaining mode to the low-voltage self-sustaining arc takes place (as described in refs. 3 and 5). This transition region is difficult to study analytically because of the difficulty in determining the proper ion current and the energy it delivers to the cathode. The energy depends on the ion accommodation coefficient, which is not well known. A much simpler situation, where the total load current is equal to zero, is discussed in the appendix.

The important parameter judging from the data in figure 6 seems to be the initial cathode temperature. There appears to be a critical initial temperature above which the discharge will begin in the non-self-sustained mode. The critical temperature in this experiment appears to be about 2135 K. To illustrate the importance of the initial temperature the following procedure was used: This time the initial electrode temperature was changed by varying the power to the arc heater. Short-circuit currents were obtained starting at low arc power with an initial cathode temperature of 1890 K. The results are shown in figure 10, where the cathode drops and corresponding temperatures against current are plotted. As the arc power is increased, the cathode temperature increases and the cathode drop decreases (curve I) from 18.0 volts at 1890 K to 10.5 volts at a cathode temperature of 2375 K. This is a typical low-voltage-arc or self-sustaining-mode discharge characteristic. While at the high arc power and cathode temperature level, the load in the circuit was changed to obtain curve II. These curves are the same as in figure 6. Thus it is possible to be either in the self-sustaining arc mode or the non-self-sustaining mode depending on the initial cathode temperature. Such transition was also observed in reference 10.

The transition from one mode into the other above the critical temperature is not well defined, and no arc spots were observed during the experiment.

The anode processes are not as complicated as the cathode because they are dominated by electron current (ref. 7). There is no cooling effect observed at the anode because the emitted electrons are braked by the anode drop.

## CONCLUSIONS

An unseeded, supersonic, nonequilibrium magnetohydrodynamic (MHD) generator using carbonized Th-W electrodes has been shown to operate in either self-supporting-arc or non-self-supporting mode depending on the initial cathode temperature. The

cathode and anode drops (losses in performance of a generator) may be reduced by operating the discharge in the non-self-supporting mode. This may be done by making sure there is sufficient thermal emission from the cathode. There is a cathode temperature ( $\sim 2250$  K) for which a minimum cathode drop is found.

Cathode and anode drops of as much as 10 and -5 volts, respectively, have been measured. The magnetic field seems not to affect the electrode drops, but appears to have some effect on cathode emission and cathode energy balance. The magnetic field also causes nonsymmetry in the potential profile. These magnetic field effects require more study.

Lewis Research Center,  
National Aeronautics and Space Administration,  
Cleveland, Ohio, September 24, 1970,  
129-02.

## APPENDIX - ZERO-CURRENT CASE

A much simpler picture presents itself at the electrodes if there is no net load current considered. This case is shown by figure 2(a) and the open-circuit conditions in figures 3 and 4. If the flux of electrons from the plasma is greater than the emitted electrons from an electrode, a field will be set up to brake the incoming electrons. This potential difference may be calculated by balancing the currents at the electrode (ref. 6)

where

$$\left. \begin{aligned} J_R &= J_e \exp \left( -\frac{e\phi}{kT_e} \right) \\ J_e &= n_e e \sqrt{\frac{kT_e}{2\pi m_e}} \\ J_R &= AT_c^2 \exp \left( -\frac{e\phi_w}{kT_c} \right) \end{aligned} \right\} \quad (1)$$

and where  $T_e$  is electron temperature,  $T_c$  is cathode temperature,  $n_e$  is electron number density,  $m_e$  is electron mass,  $\phi$  is electrode drop,  $\phi_w$  is work function, and  $A$  is the Richardson constant ( $120 \text{ A}/(\text{cm}^2)(\text{K}^2)$ ).

We also neglect the magnetic field effects and assume that ion current is zero and that  $n_e$  is in Saha equilibrium at the electron temperature. The unknowns in the equation are  $T_e$ ,  $\phi$ , and  $\phi_w$ . Using values derived from the experiment for  $\phi$  and  $\phi_w$  we may calculate the electron temperature for the zero current condition as follows: The work function is approximated by finding the current density with an initial cathode temperature of 2325 K (solid symbols, fig. 6) at the bottom of the cooling curve. At this point of the cooling curve it is assumed that saturated emission has occurred, that no ion heating effects have yet taken place, and that the drops are too small to have contributed to field emission. The current density is calculated by dividing the current by the cathode area. The work function is calculated from Richardson's equation using this current density and the measured cathode temperature. This value of work function is 3.5 eV. The cathode drop with an initial cathode temperature of 2325 K at zero discharge current is 0.75 volt. The electron temperature is then calculated from the current balance equation (eq. (1)) for these conditions and is found to be 6370 K.

Floating double-probe and spectrographic measurements (shown in fig. 11) have confirmed that the electron temperature is in this range for zero discharge current. Spectrographic measurements were done by R. J. Sovie using the standard two-line intensity ratio method and assuming local thermodynamic equilibrium. The following two-line ratios were averaged to obtain the results in figure 11: 4259/4272, 4345/4164, and 4333/4266. It was found that the electron temperature is 8000 to 9000 K and independent of arc power. As expected, the calculated electron temperature of 6370 K (near the electrode) is lower than the measured electron temperature because of the presence of the relatively cold electrode.

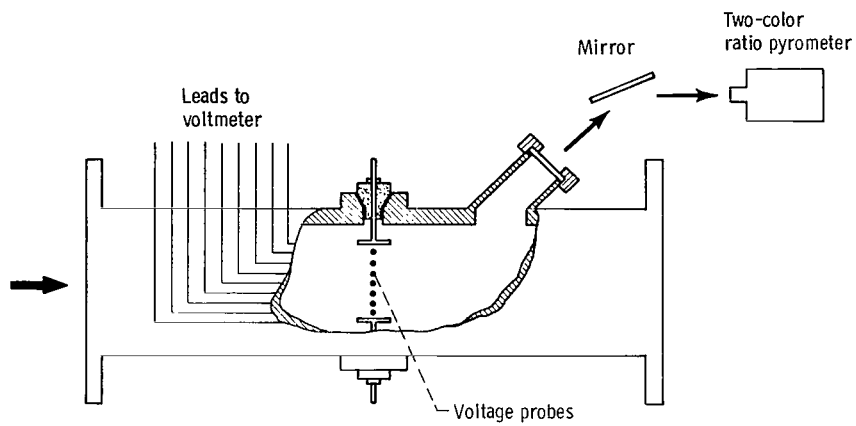
The zero-current drop affects the open-circuit distribution obtained with magnetic fields, as illustrated in figure 12. The resultant curve is similar to those for the open-circuit case in figures 3 and 4.

## REFERENCES

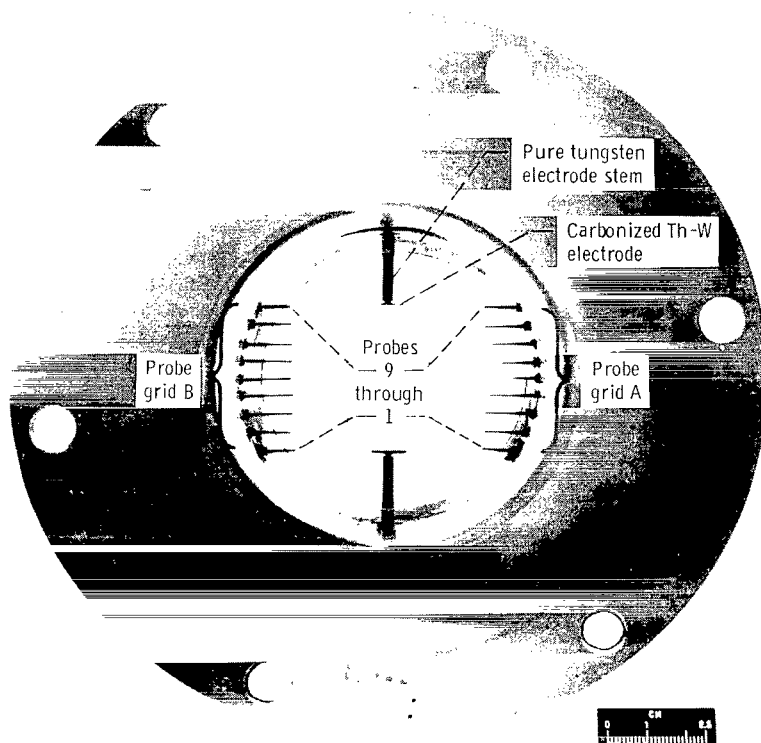
1. Kessler, R.; and Eustis, R. H.: Effects of Electrode and Boundary-Layer Temperatures on MHD Generator Performance. Ninth Symposium on Engineering Aspects of Magnetohydrodynamics. Univ. Tennessee Space Inst., 1968, pp. 33-40.
2. Mantenieks, M. A.; and Nichols, L. D.: Current-Voltage Measurements in a Supersonic MHD Generator with an Arc-Heated Argon Plasma. Engineering Developments in Energy Conversion. ASME, 1965, pp. 33-48.
3. Nichols, L. D.; and Mantenieks, M. A.: Analytical and Experimental Studies of MHD Generator Cathodes Emitting in "Spot" Mode. Paper 69-WA/HT-51, ASME, Nov. 1969.
4. Schneider, P.: Thermionic Emission of Thoriated Tungsten. J. Chem., Phys., vol. 28, no. 4, Apr. 1958, pp. 675-682.
5. Ellington, H. I.: Low Voltage Diffuse Discharge in Atmospheric Pressure Helium and Argon, Seeded with Small Amounts of Caesium, Potassium, and Sodium. Rep. AERE M-1616, United Kingdom Atomic Energy Authority, July 1965.
6. Bauer, A.: The Arc Cathode. An Introduction to Discharge and Plasma Physics. S. C. Haydon, ed., Armidale, New South Wales, 1964, p. 326.
7. Ecker, G.: Electrode Components of the Arc Discharge. Ergeb. Exakten Naturwiss., vol. 33, no. 1, 1961, pp. 1-104.
8. Musin, A. K.: Establishment of an Electrical Current in Moving Plasma Under Conditions of Thermionic Emission. High Temp., vol. 4, no. 4, July-Aug. 1966, pp. 456-464.
9. Maslennikov, N. M.; and Germanyuk, V. N.: Experimental Investigation of the Electrical Conductivity in a Stream of Argon and Potassium. High Temp., vol. 3, no. 4, July-Aug. 1965, pp. 479-484.
10. Koester, J. K.; Sajben, M.; and Zukoski, E. E.: Analytical and Experimental Studies of Thermionically Emitting Electrodes in Contact with Dense, Seeded Plasmas. Proceedings of the 11th Symposium on Engineering Aspects of MHD, 1970, pp. 54-60.
11. Kondrat'ev, F. V.; Sinyutin, G. V.; and Tikhonov, V. F.: Electron Cooling of the Cathode in Thermionic Converters. Soviet Phys. -Tech. Phys., vol. 13, no. 4, Oct. 1968, pp. 526-529.
12. Lyubimov, G. A.: Change of Electrical Potential Near Wall of Channel During Motion of Ionized Gas in Magnetic Field. J. Appl. Mech. Tech. Phys., no. 5, Sept. - Oct. 1963, pp. 33-51.

TABLE I. - PLASMA CONDITIONS

Initial electrode temperature, K	Argon flow rate, kg/sec	Argon temperature, K	Argon pressure, N/m <sup>2</sup>	Argon velocity, m/sec	Magnetic field, T
2166	0.038	730	$2.58 \times 10^3$	1690	0.54
2250	.031	840	2.46	1920	↓
2135	.053	610	2.94	1640	↓
2325	.024	940	2.37	2080	↓
2310	↓	940	↓	2030	.39
2320	↓	850	↓	1930	.54
2325	↓	850	↓	1930	.39



(a) Schematic of test section with voltage probes and pyrometer viewing port.



(b) View of test section with electrodes and probe. (Gas flow is into plane of paper.)

Figure 1. - Instrumentation of test section.

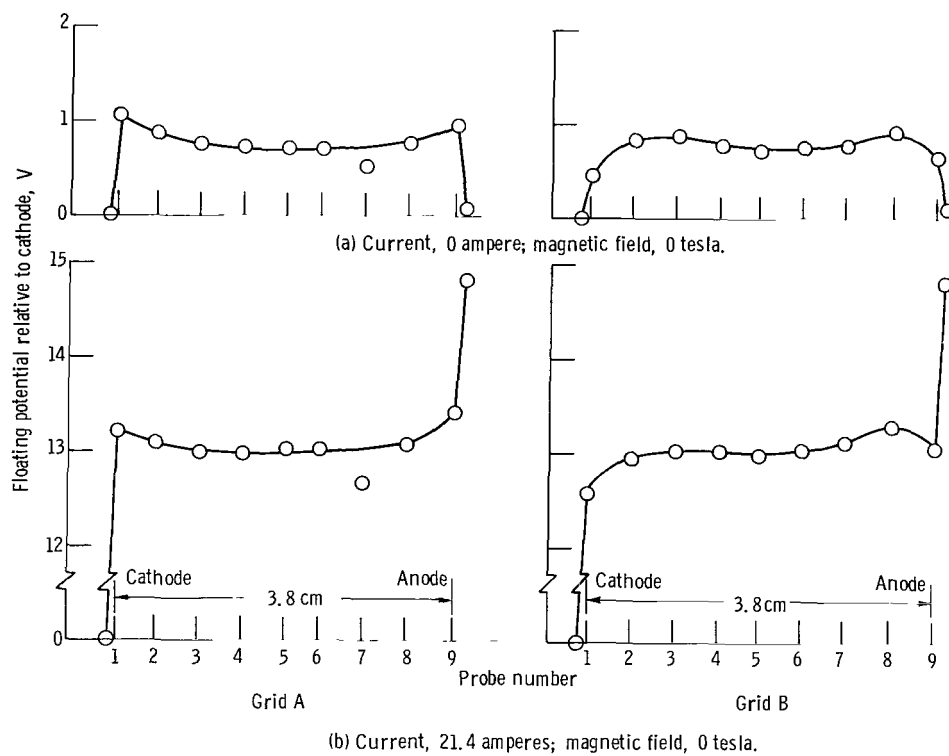


Figure 2. - Floating potential across electrode gap with no current and with applied voltage.



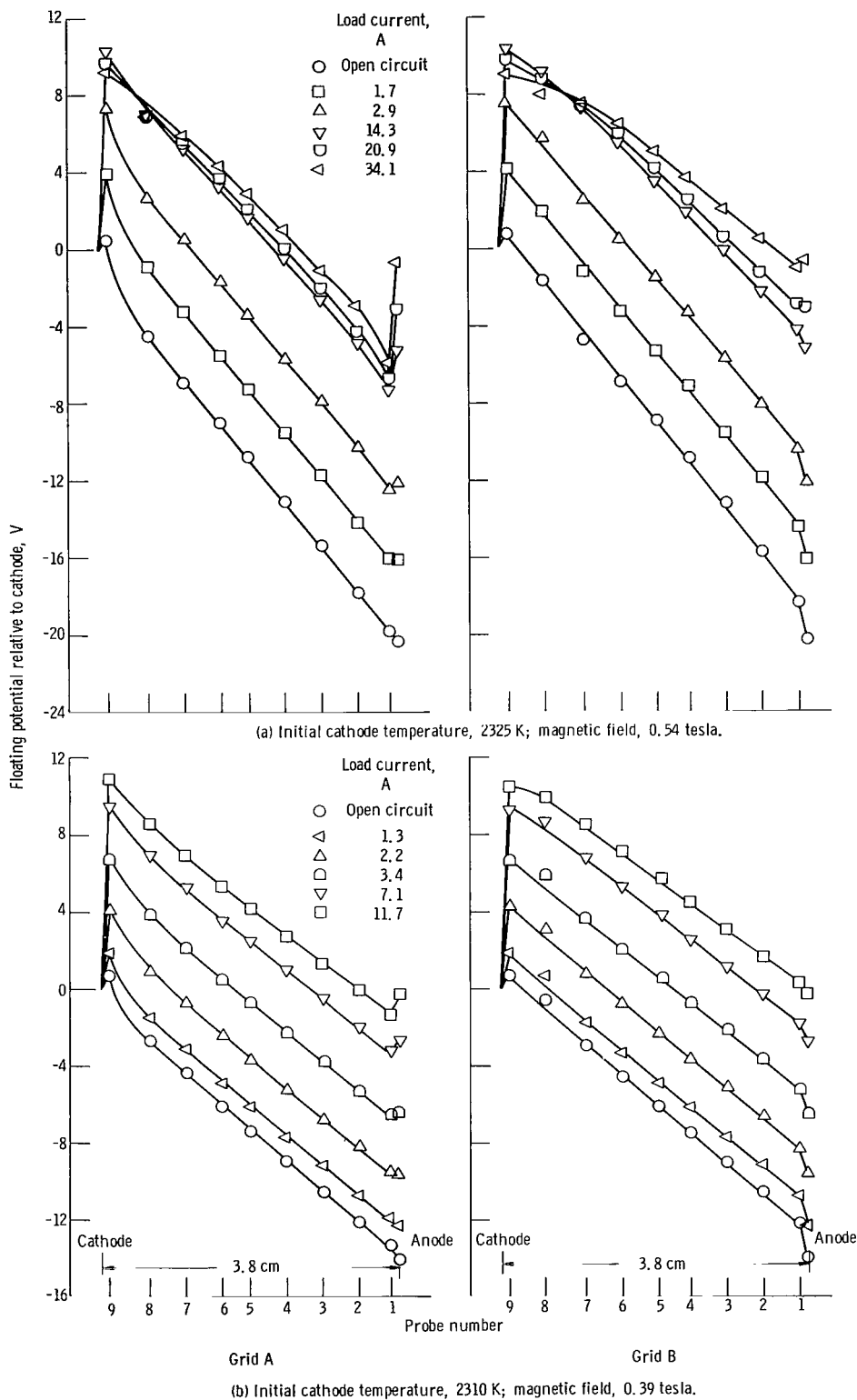


Figure 3. - Floating potential across electrode gap, top electrode as cathode. Mass flow rate, 0.024 kilogram per second; static temperature, 940 K; static pressure,  $2.37 \times 10^3$  newtons per square meter.

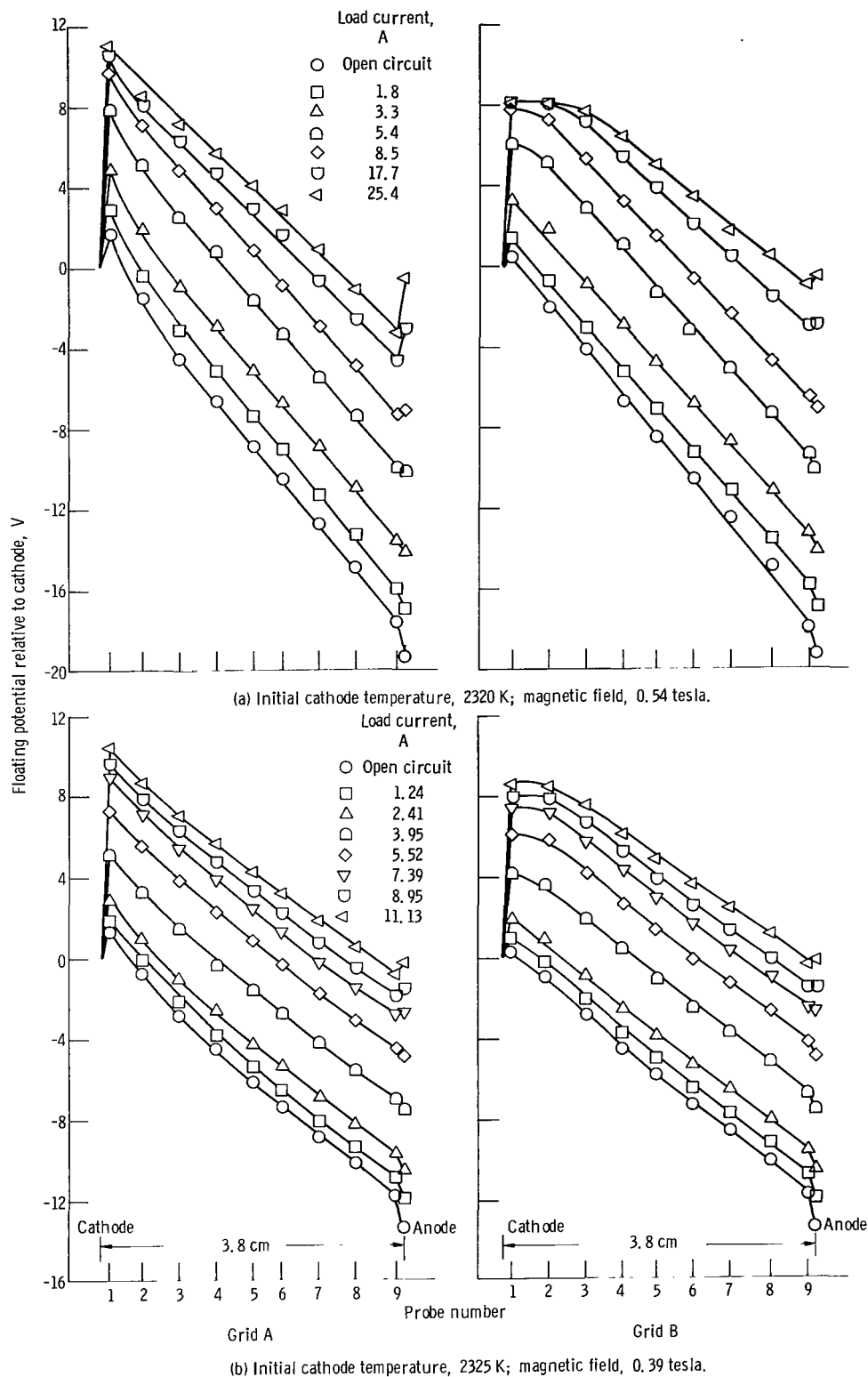


Figure 4. - Floating potential across electrode gap, bottom electrode as cathode. Mass flow rate, 0.024 kilogram per second; static temperature, 850 K; static pressure,  $2.37 \times 10^3$  newtons per square meter.

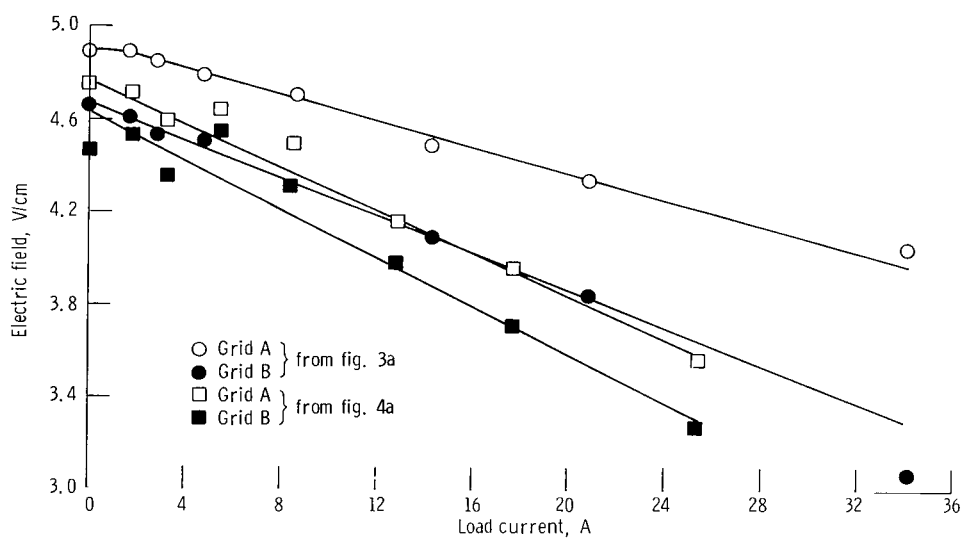


Figure 5. - Electric field in center of duct calculated from the floating potential profiles, against load current.

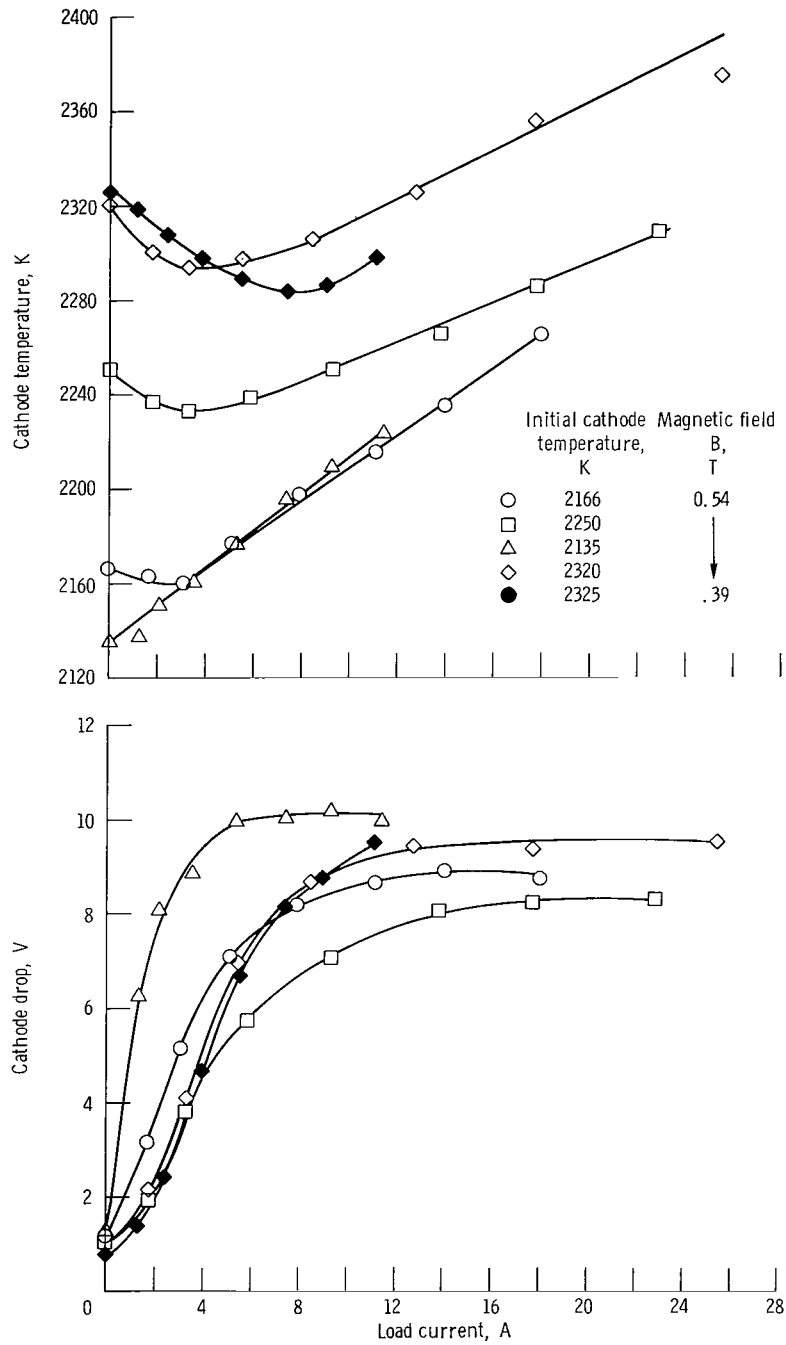


Figure 6. - Cathode drop and cathode temperature against load current, of different initial cathode temperatures.

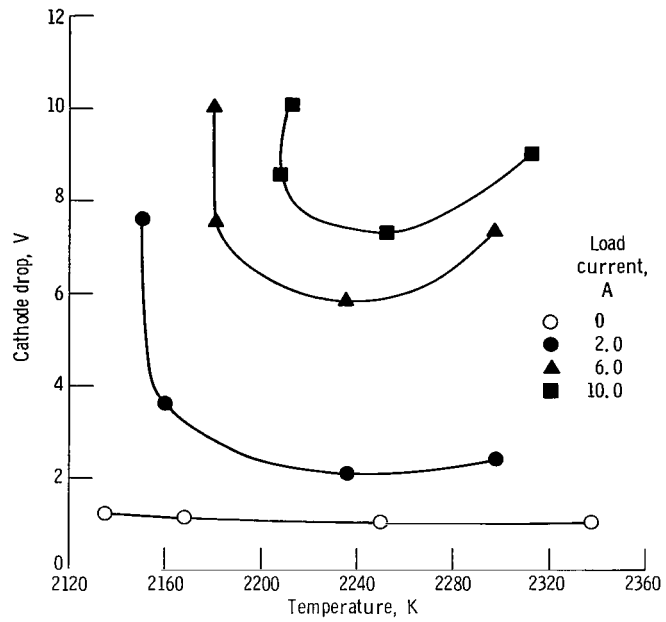


Figure 7. - Cathode temperature against cathode drop. Magnetic field, 0.54 tesla.

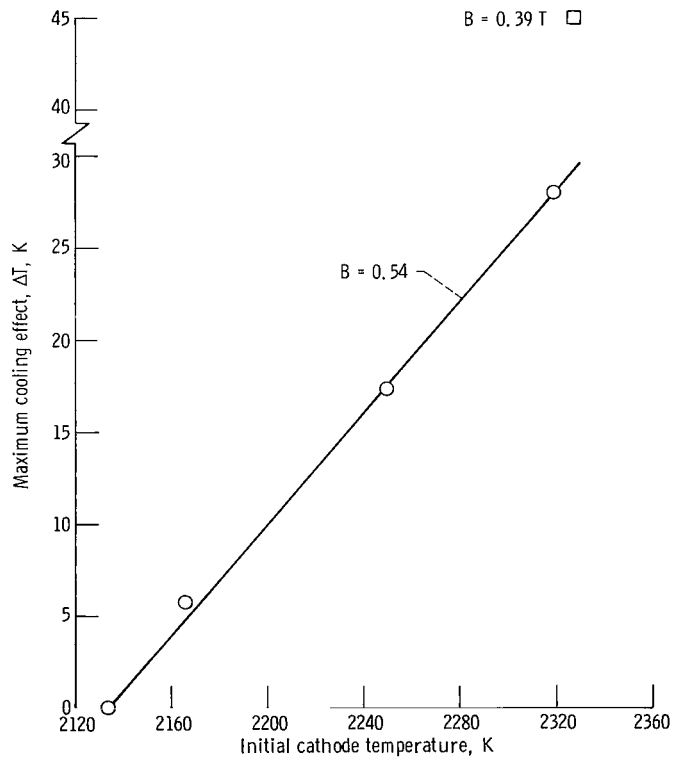


Figure 8. - Maximum cooling effect against initial cathode temperature.

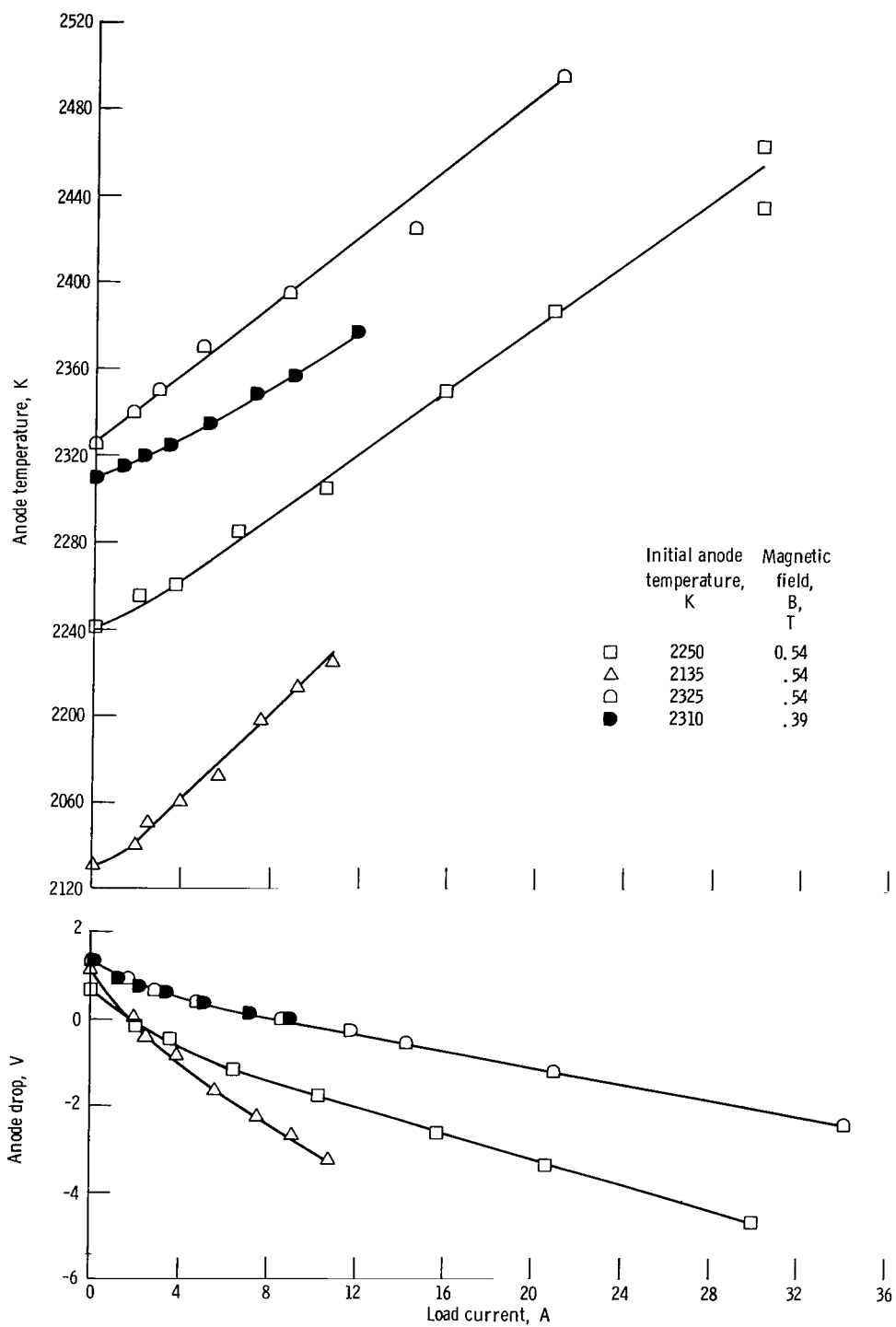


Figure 9. - Anode temperature and anode drop against load current, for different initial anode temperatures.

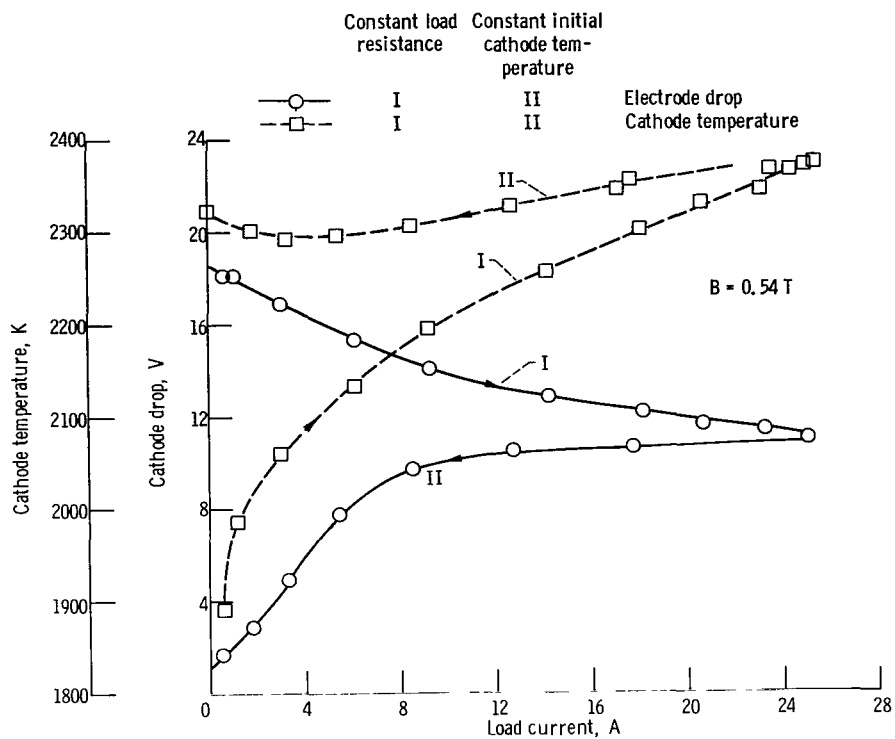


Figure 10. - Cathode drop and cathode temperature against load current, at different arc heater power levels. Grid A.

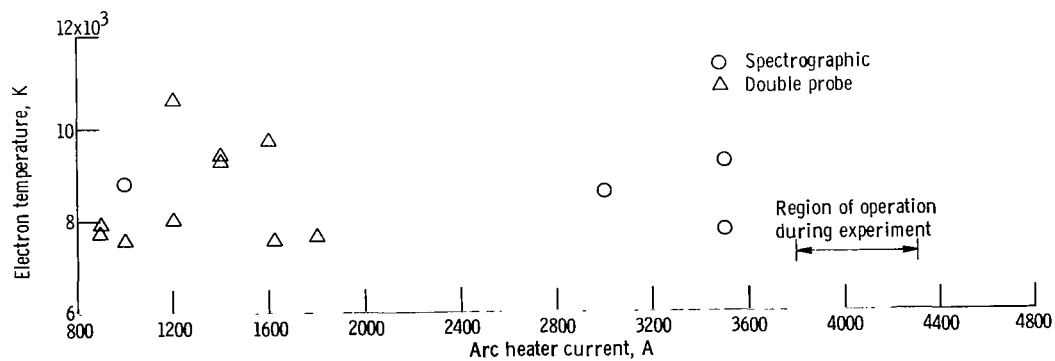
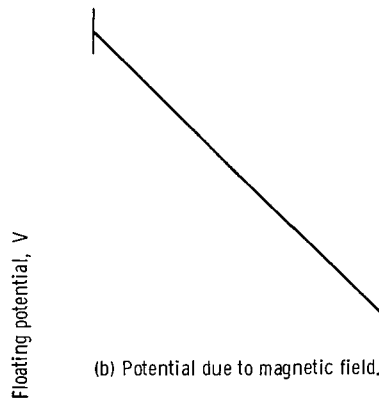


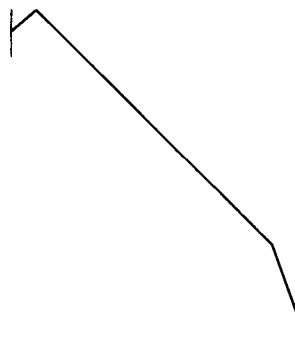
Figure 11. - Spectrographic and double-probe electron temperature measurements against arc heater current.



(a) Potential due to electron flux from plasma.



(b) Potential due to magnetic field.



(c) Result of adding potentials in parts (a) and (b).

Figure 12. - Effect of zero-current electrode drop on open-circuit voltage profile in electrode gap.



NATIONAL AERONAUTICS AND SPACE ADMINISTRATION

WASHINGTON, D. C. 20546

OFFICIAL BUSINESS

FIRST CLASS MAIL



POSTAGE AND FEES PAID  
NATIONAL AERONAUTICS AND  
SPACE ADMINISTRATION

03U 001 50 51 3DS 71012 00903  
AIR FORCE WEAPONS LABORATORY /WL0L/  
KIRTLAND AFB, NEW MEXICO 87117

ATT E. LOU BOWMAN, CHIEF, TECH. LIBRARY

POSTMASTER: If Undeliverable (Section 15  
Postal Manual) Do Not Return

*"The aeronautical and space activities of the United States shall be conducted so as to contribute . . . to the expansion of human knowledge of phenomena in the atmosphere and space. The Administration shall provide for the widest practicable and appropriate dissemination of information concerning its activities and the results thereof."*

—NATIONAL AERONAUTICS AND SPACE ACT OF 1958

## NASA SCIENTIFIC AND TECHNICAL PUBLICATIONS

**TECHNICAL REPORTS:** Scientific and technical information considered important, complete, and a lasting contribution to existing knowledge.

**TECHNICAL NOTES:** Information less broad in scope but nevertheless of importance as a contribution to existing knowledge.

**TECHNICAL MEMORANDUMS:** Information receiving limited distribution because of preliminary data, security classification, or other reasons.

**CONTRACTOR REPORTS:** Scientific and technical information generated under a NASA contract or grant and considered an important contribution to existing knowledge.

**TECHNICAL TRANSLATIONS:** Information published in a foreign language considered to merit NASA distribution in English.

**SPECIAL PUBLICATIONS:** Information derived from or of value to NASA activities. Publications include conference proceedings, monographs, data compilations, handbooks, sourcebooks, and special bibliographies.

**TECHNOLOGY UTILIZATION PUBLICATIONS:** Information on technology used by NASA that may be of particular interest in commercial and other non-aerospace applications. Publications include Tech Briefs, Technology Utilization Reports and Technology Surveys.

*Details on the availability of these publications may be obtained from:*

**SCIENTIFIC AND TECHNICAL INFORMATION OFFICE**

**NATIONAL AERONAUTICS AND SPACE ADMINISTRATION**

**Washington, D.C. 20546**